DESIGN OF A PI/2 MODE S-BAND LOW ENERGY TW ELECTRON LINEAR ACCELERATOR

S. H. Shaker*, School of Particle and Accelerators, IPM, Tehran, Iran ; CERN, Geneva, Switzerland
F. Ghasemi#, Shahid Beheshti University (sbu) Radiation Application Department, Tehran, Iran

Abstract

This design is related to a Pi/2 mode S-Band low energy TW electron linear accelerator which is in the construction stage. This project is supported by the school of particles and accelerators, institute for research in fundamental sciences (IPM), Tehran, Iran. This design consists of a buncher and an accelerating structure that are joined and two couplers for the input/output feedings. At each design stage, different methods (analytical or numerical) are used to confirm the results and also to have a better understanding.

INTRODUCTION

Figure 1 shows the layout of this Linac. The thermionic electron gun produces a continuous beam with 45 keV (β_e =0.39) kinetic energy and 1 mA current. Inside the buncher, the beam is bunched and accelerated up to 1.4 MeV and 68% of the beam is captured. Then inside the accelerating structure, the electrons are accelerated up to 8.25 MeV. Both structures are electrical-coupling disk-loaded waveguide structures. The buncher is a tapered structure, which allows the increasing of phase velocity along its length from 0.5c to 1.0c. The accelerating structure is a constant-impedance structure with the phase velocity equals to 1.0c. These two structures are designed and tuned by Superfish code and also the result is confirmed by two analytical methods by E.L. Chu et al. [1] and J. Gao [2]. Also, a code in MATLAB is written for the beam-tracking inside these two structures. The couplers are designed by HFSS code. Two different methods are used to tune the couplers, one by measuring the coupling coefficient between the couplers and their joined waveguides [3] and another one by measuring the cell to cell phase advance [4].

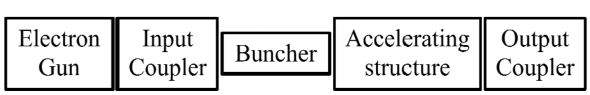

Figure 1: Linac layout.

ACCELERATING STRUCTURE

The accelerating structure is a constant-impedance structure that means all cells are similar. Figure 2 shows two cells (one plus two half cells). The cell to cell phase advance is 90°. The pi/2 mode was chosen because historically, the initial design was based on the SLAC Mark III [5]. The length of accelerating structure is 120 cm that consists of two 60 cm structures with 24 cells (23 cells + two half cells on both sides). In Table 1 you can find the values was chosen for the cell parameters.

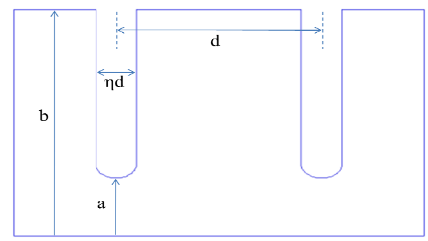

Figure 2: Cell layout.

Table 1: Cell Parameters

a	10 mm
d	25 mm
ηd	5 mm(η=0.2)
Phase velocity/c (β_w)	1
Guide wave length (λ_g)	$(2\pi/(\pi/2))$d=100 mm
Free space wave length (λ_0)	λ_g / β_w =100 mm
Resonant frequency	2997.92 MHz

The b (see Fig. 2) was found to be 39.252 mm using the Superfish code. The Superfish model is chosen similar to Fig. 2. Also two different analytical methods are used to confirm this result. In the first method the b is calculated by equation 1 [1]. The b, by this equation is equal to 39.255 mm (0.008 % difference).

$$(1)\quad \begin{cases} \dfrac{1}{k_r a}\dfrac{J_1(k_r a)}{J_0(k_r a)} = \dfrac{1}{(1-\eta)ka}\dfrac{J_1(ka)N_0(kb) - N_1(ka)J_0(kb)}{J_0(ka)N_0(kb) - N_0(ka)J_0(kb)} \\ k = \dfrac{2\pi}{\lambda_0}, k_z = \dfrac{2\pi}{\lambda_g} = \dfrac{2\pi}{\beta_w \lambda_0}, {k_r}^2 = k^2 - {k_z}^2 \end{cases}$$

Another method is from J.Gao [2]. In this method, each cell is replaced by a pillbox and the two coupling holes of the cell are replaced by the equivalent electric dipoles. Equation 2 shows how to calculate the resonant frequency by this method. The $\omega_0/2\pi$, E_0 and U are the resonant frequency, the maximum axial electric field and the average stored energy of the pillbox (cell without holes) in TM_{010} mode, respectively. The radius of this pillbox is equal to b and its length is equal to d(1- η). The b, by this equation was found to be 39.240 mm (0.03 % difference).

$$(2)\quad \begin{cases} \omega_{\frac{\pi}{2}} = \omega_0 \sqrt{1 + \dfrac{2}{3}\varepsilon_0 a^3 \dfrac{{E_0}^2}{U}} = \dfrac{x_{01}c}{b}\sqrt{1 + \dfrac{{}^4/_{3\pi}}{J_1^2(x_{01})}\dfrac{{}^{a^3}/_{b^2 d}}{(1-\eta)}} \\ x_{01} \approx 2.4048 \text{ (First root of } J_0 \text{ function)} \end{cases}$$

*hamed.shaker@cern.ch ; shaker@ipm.ir
#farshad.ghasemi@gmail.com

Calculating the Axial Electric Field

Equation 3 [6] introduces the axial electric components inside the accelerating structure. Just, the n=0 component is contributed in the acceleration process because the phase velocity of this component and the beam velocity is equal (β_w=β_e=1). Other components aren't contributed in the acceleration process but they carry the energy. By knowing the total axial electric field by Superfish, a_n's for each component is calculated using equation 3 for the SW case. a_0 and a_{-1} were found to be 0.885 MV/m and 0.206 MV/m, respectively. The other components are less than 0.015 MV/m. These values are normalized values because in the Superfish, the average axial electric field is normalized to 1 MV/m.

$$(3)\begin{cases} E_{z,TW}(r,z) = \sum_{n=-\infty}^{n=+\infty} a_n J_0(k_{rn}r)e^{i(k_{zn}z-\omega t)} \\ E_{z,SW}(0,z) = e^{-i\omega t}\sum_{n=-\infty}^{n=+\infty} 2a_n \cos(k_{zn}z) \\ k_{zn}d = \frac{\pi}{2}+2\pi n \end{cases}$$

Equation 4 shows how to calculate the real axial electric field for the main component. P_{TW} [6] is equal to the normalized transmission power from a surface perpendicular to the axis and is calculated from the Superfish result. In equation 4 this surface is located at the middle of the disk hole. The real transmission power is equal to the input power (2 MW) if there is no power loss inside the structure and the couplers are matched.

$$(4)\begin{cases} E_{z,TW} = a_0\sqrt{\frac{2MW}{P_{TW}}} = a_0\sqrt{\frac{2MW}{26461W}} \approx 7.44\ MV/m \\ P_{TW} = \frac{1}{4}\int_0^a E_{r,SW}\left(r,\frac{d}{2}\right)H_{\varphi,SW}(r,\frac{d}{2})2\pi r dr \end{cases}$$

BUNCHER

The buncher has 15 cells (14 plus two half cells on both sides) and its length is 30.8 cm. The phase velocity (β_wc) of cells should be increased to reach 1.0c for the last cell. Figure 3 shows the phase velocities was chosen for the buncher cells. The last 2.5 cells (two plus one half cells) are similar to the accelerating structure cells. The disk hole radius (a in Fig. 2) and the disk thickness (ηd in Fig. 2) for each cell is similar to the accelerating structure cells. Now by using equation 5 [5], we can find the main component axial electric field (E_0) inside of each cell. Figure 4 shows the axial electric field inside the buncher and the accelerating structure. The red (blue) line shows the electric field when the power loss due to the finite wall conductivity (copper) is (isn't) considered. The internal radius (b in Fig. 2) for each cell was found by using equation 1 and was corrected by the Superfish code.

$$(5)\begin{cases} \frac{a^4\alpha^2}{\beta_w}f(k_r a) = constant\ ;\ \alpha = \frac{E_0 e\lambda_0}{m_0c^2} \\ f(k_r a) = \frac{8}{(k_r a)^2}[J_1{}^2(k_r a) - J_0(k_r a)J_2(k_r a)] \end{cases}$$

Figures 5 and 6 show the different particle trajectories inside the structure (the buncher and the accelerating structure) with different initial relative phase. These trajectories are calculated by the equation 6 [5]. Figure 5 shows that 68% of the continuous beam (244°) is captured and is focused to about 15°. Figure 6 shows the final energy is equal to 8.25 MeV and the energy spread is 0.26 MeV (3.1 %).

$$(6)\begin{cases} \frac{d\Delta}{d\xi} = 2\pi\left(\frac{1}{\beta_w}-\frac{1}{\beta_e}\right);\ \xi = \frac{z}{\lambda_0} \\ \frac{d\gamma}{d\xi} = -\alpha\sin(\Delta)\ ;\ \gamma = \frac{1}{(1-\beta_e{}^2)^{\frac{1}{2}}} \end{cases}$$

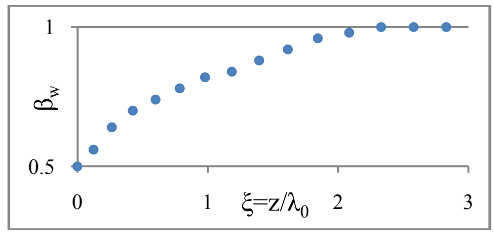

Figure 3: Phase velocity/c of each buncher cell.

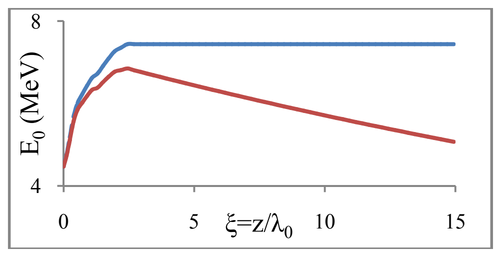

Figure 4: Maximum axial electric field.

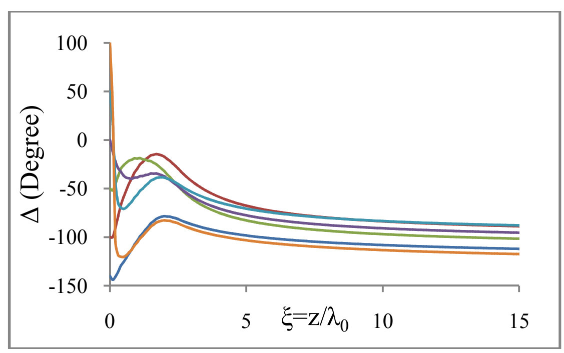

Figure 5: Relative phase evolution of different particles.

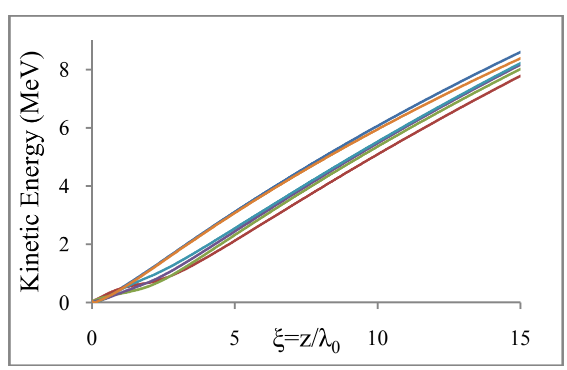

Figure 6: Kinetic energy evolution of different particles.

INPUT/OUTPUT COUPLERS

There are two couplers. The input coupler is located at the beginning of buncher and the output coupler is located at the end of accelerating structure. Figure 7 shows the couplers layout. Two methods were used to tune the couplers. The goal of tuning methods is to find R_c and L_s to reach to the minimum reflection from input coupler and to have pure traveling wave inside the structure as much as possible for our working frequency (2997.92 MHz). Each coupler cell is different from the joined cells and is connected to a WR-284 waveguide via a tapered structure waveguide. R_p is equal to 7.5 mm/10 mm and L_c is equal to 9 mm/20 mm for the input/output coupler. The nose cone that is shown in Fig. 7 is just for the input coupler to avoid the SW fields for the first half of the coupler cell [7].

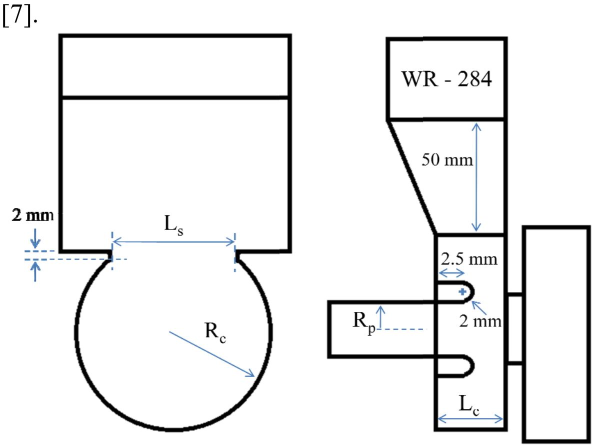

Figure 7: Coupler layout.

In the first method [3] the coupler is detuned by an external conductor object (PEC in our simulation) and the reflection angles are measured for two different frequencies near our working frequency. Then, the first joined cell is detuned and again the reflection angles are measured for the same frequencies. By using equation 7 [3], the resonant frequency of coupler cell (ω_c) and coupling coefficient (β) between the coupler cell and the waveguide are calculated. $\varphi_{1,2}$ is equal to the difference between reflection angles for the first joined detuned and the coupler cell detuned cases for each chosen frequency. In this equation, k comes from the dispersion equation and is equal to 0.0225/0.0147 for the joined cells of input/output coupler and $\theta_0=\pi/2$ for our structure. The coupler is matched when $\omega_c=\omega_{\pi/2}=2997.92$ MHz and $\beta=1$ (see Table 2).

$$
(7)\begin{cases}
\omega_c = \sqrt{\omega_1\omega_2}\sqrt{\dfrac{\omega_2\tan\left(\frac{\varphi_2}{2}\right)-\omega_1\tan\left(\frac{\varphi_1}{2}\right)}{\omega_1\tan\left(\frac{\varphi_2}{2}\right)-\omega_2\tan\left(\frac{\varphi_1}{2}\right)}} \\
\beta = \dfrac{1}{\frac{k}{2}\omega_{\frac{\pi}{2}}\sin(\theta_0)}\dfrac{\tan\left(\frac{\varphi_1}{2}\right)\tan\left(\frac{\varphi_2}{2}\right)(\omega_1^2-\omega_2^2)}{\omega_1\tan\left(\frac{\varphi_2}{2}\right)-\omega_2\tan\left(\frac{\varphi_1}{2}\right)} \\
\omega_{\theta_0} = \omega_{\frac{\pi}{2}}\left(1-\frac{k}{2}\cos(\theta_0)\right) \text{ : dispersion equation}
\end{cases}
$$

In the second method [4] the difference between reflection angles is measured when a conductor plate is placed at the middle of the different joined cells. The coupler is matched when the reflection angles difference for the working frequency is 180° (2 × 90°) for moving the plate by one cell (see Table 2). The angles are indicated in this table are the phase advance between the first and second joined cells and between the second and third joined cells. These angles are the best result for our machining accuracy (0.01 mm). Based on the results of these two methods, the final values for the construction are chosen in a manner that gives us the flexibility during experimental tuning process. L_s can be extended a little by cutting and sanding the slot and the resonant frequency can be tuned by small mechanical deforming of coupler cell wall. To deform, we need a few holes around the cell to drill up to inner wall to make a thin wall layer.

Table 2: R_C and L_s

Coupler/Method	R_C	L_s
Input / 1	34.73 mm	28.4 mm
Input / 2 (89.1°,87.2°)	34.81 mm	28.5 mm
Input / Final	34.81 mm	28.3 mm
Output / 1	38.59 mm	26.55 mm
Output / 2 (89.4°,81.6°)	38.575 mm	26.55 mm
Output / Final	38.61 mm	26.4 mm

REFERENCES

[1] E. L. Chu and W. W. Hansen, "The Theory of Disk Loaded Wave Guides", J. Appl. Physics, November 1947, Vol. 18, p. 996 -1008.

[2] J. Gao, "Analytical Approach and Scaling Laws in the Design of Disk-Loaded Travelling Wave Accelerating Structures", Particle Accelerators, 1994, Vol. 43(4), p. 235-257.

[3] S. Zheng et al., "A Quantitative Method of Coupler Cavity Tuning and Simulation", PAC01 Proceedings, June 2001, p. 981-983; http://www.JACoW.org .

[4] D. Alesini et al., "Design of couplers for traveling wave RF structures using 3D electromagnetic codes in the frequency domain", Nucl. Instrum. Methods A, June 2007, 580 (2007), p. 1176-1183.

[5] M. Chodorow et al., "Stanford High-Energy Linear Electron Accelerator(Mark III)", Rev. Sci. Instrum., February 1955, Vol. 26(2), p. 134-204.

[6] G. A. Loew et al., "Computer Calculations of Travelling Wave Periodic Structure Properties", SLAC-PUB-2295, March 1979 (A).

[7] J. Haimson, "Electron Bunching in Traveling Wave Linear Accelerators", Nucl. Instrum. Methods, January 1966, Vol. 39(1), p. 13-34.